Available online at www.sciencedirect.com
ScienceDirect
Progress in Natural Science: Materials International 21(2011) 485−490
Progress in Natural Science: Materials International
www.elsevier.com/locate/pnsc

Influence of stacking fault energy on formation of long period stacking ordered structures in Mg−Zn−Y−Zr alloys

Fu-sheng PAN[1, 2], Su-qin LUO[1], Ai-tao TANG[1, 2], Jian PENG[1, 2], Yun LU[3]
1. College of Materials Science and Engineering, Chongqing University, Chongqing 400044, China;
2. National Engineering Research Center for Magnesium Alloys, Chongqing University, Chongqing 400044, China;
3. Faculty of Engineering, Chiba University, Chiba 263-8522, Japan

Received 30 November 2011; accepted 15 December 2011

Abstract: The influence of alloying elements on the stacking fault energy (SFE) of Mg−Y−Zn−Zr alloys was calculated by using first-principles, and the microstructure of as-cast Mg-1.05Y-0.79Zn-0.07Zr (mole fraction, %) alloy prepared by conventional casting was investigated by SEM, TEM and HRTEM. The block-like long period stacking ordered (LPSO) phase, the lamellar LPSO phase and stacking faults were observed simultaneously and the lamellar LPSO structure and stacking faults were both formed on $(0001)_{\alpha\text{-Mg}}$ habit plane and grown or extended along $[01\bar{1}0]_{\alpha\text{-Mg}}$ direction. The calculation results by the first-principles showed that the addition of Y can sharply decrease the stacking fault energy of the Mg−Zn−Y−Zr alloy, while Zn slightly increases the stacking fault energy of the alloy. The influence of stacking fault energy on the formation of LPSO was discussed. It shows that LPSO may nucleate directly through stacking faults and the lower stacking fault energy was in favor of formation of LPSO.
Key words: magnesium alloy; Mg−Zn−Y−Zr; long period stacking ordered (LPSO) structures; stacking fault energy (SFE); first-principles calculation

1 Introduction

As the lightest metal structural materials, magnesium alloys are being used to speed up the application of lightweight parts in automotive, motorcycle and aerospace fields due to their high specific strength, stiffness and low density [1]. Re additions were reported to have great effects on the microstructure and mechanical properties of magnesium alloys [2−9]. In recent years, the Mg−Zn−Re alloys containing long period stacking ordered (LPSO) structures have been the focus of attention due to their unique microstructures and excellent mechanical properties [7−19]. The tensile yield strength of such alloys could reach as high as 610 MPa, while keep not less than 5% for the elongation at ambient temperature when the alloy ($Mg_{97}Zn_1Y_2$) was produced by rapid solidification processing [20]. The hot compressive peak stress at 573 K was about 190 MPa, compared with the value of 72 MPa for ZK60 alloy, and no macroscopic fracture took place up to a strain of about 60% in Mg97Zn1Y2 alloy prepared by high frequency induction melting [18]. Warm-extruded Mg96.5Zn1Gd2.5 (mole fraction, %) alloys with LPSO structure exhibited high tensile yield strength (345 MPa) and large elongation (6.9%), due to the refinement of α-Mg grains and the high dispersion of a hard LPSO structure phase [21]. These excellent properties were considered to be contributed not only by grain refinement but also a novel precipitate with a LPSO structure [22]. Furthermore, it has been reported that the LPSO structure prohibits the deformation twin of the 2H-Mg matrix.

According to the reports, the LPSO phase can be divided into two types in terms of the morphology and the distribution of LPSO structure in the Mg−Zn−Y alloy. The first one was as the block-like primary phase found at the grain boundaries in ingots produced by conventional casting [23], the other one was as a precipitate observed inner the α-Mg solid solution grains in the rapid solidified powder after hot extrusion [22]. However, the corresponding formation mechanism of different types of LPSO structure still remained unclear. As for the second type, ABE et al [22] pointed out that the corresponding transformation can be accomplished via two processes: introducing the stacking faults on

Foundation item: Project (50725413) supported by the National Natural Science Foundation of China; Project (2010CSTC-BJLKR) supported by the Chongqing Science and Technology Commission of China
Corresponding author: Fu-sheng FAN; Tel: +86-23-65112635; E-mail: fspan@cqu.edu.cn

every six close-packed planes in the α-Mg structure for stacking ordering, and supplying the solute Zn and Y atoms to and adjacent to the faulting layers for chemical ordering. Unfortunately, ABE et al [22] did not give the confirmable demonstration to the stacking faults and the deep-seated reason why the stacking faults can be formed easily in the alloy. As we know, the lower the stacking fault energy (SFE) of the alloy is, the more probably the stacking faults are formed. Therefore, it is necessary to evaluate the SFE of the Mg−Zn−Y−Zr alloy.

The relationship among stacking faults, stacking faults energy and formation of LPSO structure in Mg−Zn−Y−Zr alloys was investigated by experiments and first-principles calculation within the framework of density functional theory. In order to explore the stacking faults mechanics for the formation of LPSO structure, firstly, we focused on the question whether the alloying elements Y and Zn can decrease the SFE of Mg−Zn−Y−Zr alloy. Because of lack of the experimental results of the SFE, first principles calculation known as a reliable tool was chosen to estimate the influence of alloying elements Y and Zn on the SFE. Secondly, experimental investigations were conducted to reveal the relationship between stacking faults and LPSO structure. Finally, we went in detail into the formation mechanics of the LPSO and tried to explore the influence of SFE on formation of LPSO structure.

2 Experimental

The analyzed chemical composition of the alloy used in this study was Mg-1.05Y-0.79Zn-0.07Zr (mole fraction, %). The alloy ingot with size of 90 mm in diameter and 200 mm in length was prepared from high purity Mg (99.9%), purity Zn (99.9%), Mg-30Y (mass fraction, %) master alloy and Mg-31Zr (mass fraction, %) master alloy in a carbon crucible under the protection of a mixed atmosphere of SF_6 (10%, volume fraction) and CO_2 (Bal.). When the melt was stirred equably and held for 10 min, it was poured into a permanent steel mould which was pre-heated to 300 °C and then cooled in air. In order to obtain a slower cooling rate, the wall thickness of the steel mould was selected to be no more than 5 mm. The microstructure of the alloy was investigated using X-ray diffraction (XRD) (Dmax−1200VBX), scanning electron microscopy (SEM) (Philips XL30) and transmission electron microscopy (TEM) with a Zeiss LIBRA 200 FE TEM under an accelerating voltage of 200 kV.

TEM specimens were prepared by the twin-jet polishing technique using a solution of 5.3 g LiCl, 11.16 g $Mg(ClO_4)_2$, 500 mL methanol and 100 mL 2-butoxy-ethanol at about −50 °C and 90 V. Ion milling with the ion beam at a lower angle to the surface was applied to remove oxide films and contaminations on the two surfaces of perforated specimens.

3 Results

3.1 Model and computation methods

The first-principles total-energy calculations were performed using a pseudopotentials method based on DFT. All calculations were performed with VASP [24]. The Perdew-Wang 91 GGA [25] and the projector augmented wave (PAW) method [26] were used. After the convergence tests, k-point mesh of 12×12×3 was adequate for good convergence and the energy cutoff of 350 eV yielded well converged results. The total-energy calculation was performed until the total energy changed within 10^{-5} eV/atom and the Hellmann-Feynman force on all atomic sites was less than10^{-2} eV/Å.

For evaluating the influence of addition of alloying elements on the SFE, the SFE surface for basal plane of pure Mg was firstly calculated, as shown in Fig. 1. A single plane of Mg was displaced in the basal plane by a linear combination of $a/3[\bar{1}\,\bar{1}20]$ and $a[\bar{1}100]$; the defected geometry was allowed to relax in the [0001] directions, and the energy per area for the defect was the SFE. Calculations were carried out using a 1×1×6 supercell corresponding to 12 basil planes ABABABABABAB. In order to model the I_2-type stacking fault, we imposed an extra $a/3[10\bar{1}0]$ component to the supercell vector along the [0001] direction above a plane B, so that the stacking sequence turned to be ABABABCACACA. The highlighted point of $a/3[10\bar{1}0]$ was a metastable configuration known as the intrinsic I_2 stacking fault, as shown in Fig. 1. The calculated results of the SFE surface for basal plane of pure Mg showed good agreement with other density functional theory calculations [27−29]. Even the calculated I_2 intrinsic SFE γ_{I_2} (45 mJ/m^2, corresponding 25 meV energy change per 1×1×6 supercell) agreed well with the experimental result (23 meV)) [27]. All these reliable calculations of the SFE for pure Mg laid a good

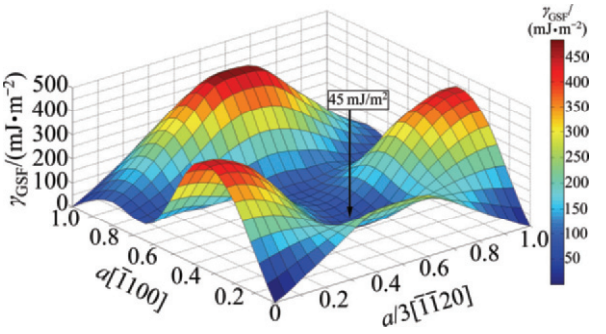

Fig. 1 Generalized stacking fault energy surface for basal plane of Mg from first-principles calculation

foundation for evaluating the influence of alloying elements on the SFE.

In order to evaluate the influence of alloying elements on the SFE, the I_2-type stacking fault was introduced into a 2×2×6 Mg supercell (*k*-point mesh of 6×6×3). The solute was substituted into a site in the stacking faults, and all the atoms were relaxed without any constraints to find a minimum energy until forces were less than 10^{-2} eV/Å. Since the configuration of I_2-type stacking fault was meta-stable, as shown in Fig. 1, it didn't need any constraints on the relaxation.

3.2 Influence of alloying elements on SFE

The calculation process for the additions of different amount needs to take very long time by the first principles. The addition of 2.08% (mole fraction) alloy element was found to a good choice for the calculation of SFE. Table 1 showed the calculated SFE of Mg with addition of 2.08% Y or Zn. The calculated value of SFE for pure Mg was 45 mJ/m^2, and addition of 2.08% Y sharply decreased the SFE of the alloy from 45 mJ/m^2 to 35 mJ/m^2 by 22.2%. And the addition of 2.08% Zn just slightly increased the SFE from 45 mJ/m^2 to 45.3 mJ/m^2 by 0.67%. However, at present there has been no experimental report about the quantitative influence of alloying elements on the SFE. In order to validate the calculated value of the SFE with addition element, the chemical misfit (ε_{SFE}) was calculated from the supercell energies as [29]:

$$\varepsilon_{SFE}=\frac{E_{displaced}(solute)-E_{undisplaced}(solute)-2\sqrt{3}a^2\gamma_{I_2}}{\gamma_{I_2}\sqrt{3}a^2/2} \quad (1)$$

where the "displaced" and "undisplaced" geometries corresponded to the supercell with and without an I_2 intrinsic stacking fault, and $\sqrt{3}a^2/2$ was the basal plane area. The term $E_{displaced}$(solute)−$E_{undisplace}$(solute) represented the interfacial energy introduced by the stacking faults. ε_{SFE}>0 indicated that the alloying element can increase the SFE, and vice versa. It was shown that the calculated ε_{SFE} with alloying element in this work agreed well with those reported by YASI et al [29]. Therefore, we can get that the addition of Y can sharply decrease γ_{I_2} of the Mg−Zn−Y−Zr alloy while Zn slightly increases γ_{I_2} of the Mg−Zn−Y−Zr alloy. Therefore, lots of stacking faults were more likely to be formed in the used alloy.

3.3 Formation of LPSO accompanied by stacking faults

Figure 2 showed the microstructure of the as-cast Mg-1.05Y-0.79Zn-0.07Zr (mole fraction, %) alloy. As shown in the SEM images, the block-like primary phase was discontinuously distributed along grain boundaries. The selected area electron diffraction (SAED) pattern ($B=[2\bar{1}\bar{1}0]_{\alpha\text{-Mg}}$) of the block-like primary phase showed that it had a 18R-type LPSO structure, with the distinct characteristic of 5 extra spots spacing equally between the central spot and the $(0001)_{\alpha\text{-Mg}}$ spot. Almost all of this block-like LPSO structure belonged to the first type of LPSO structure. A fine bright lamellar structure was observed to be formed on specific habit plane of α-Mg grains, some of which even penetrated throughout the α-Mg grains. EDS results showed that there was

Table 1 Calculated SFE of Mg alloy with addition of 2.08% Y or Zn (mole fraction)

Element	$\gamma_{I_2}/(mJ\cdot m^{-2})$	$\frac{\Delta\gamma_{I_2}}{\gamma_{I_2}}$/%	ε_{SFE}	
			This work	In Ref. [29]
Mg	45.0	0	—	—
Y	35.0	−22.2	−0.88	−1.70
Zn	45.3	+0.67	+0.04	+0.32

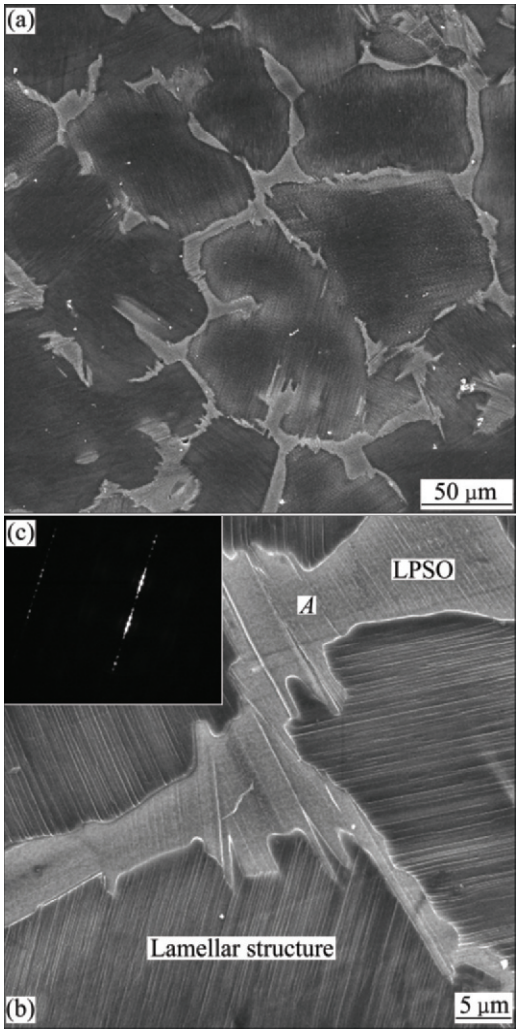

Fig. 2 Microstructures of as-cast alloy: (a), (b) SEM images; (c) Selected area electron diffraction (SAED) pattern of area *A*

segregation of Y and Zn around the area of this kind of lamellar structure.

In order to clearly make this kind of fine lamellar structure and the orientation relationship between the lamellar structure and α-Mg matrix, the lamellar structure was carefully observed by TEM and HRTEM. Figure 3 showed the TEM bright field image of the lamellar structure. It could be found that the width of the lamellar structure was not uniform and it ranged from about 2 to 20 nm.

Figure 4 showed the HRTEM image and FFT pattern of the lamellar structure with width over 5 nm. The FFT pattern ($B=[2\bar{1}\bar{1}0]_{\alpha\text{-Mg}}$) showed that it also had a 18R-type LPSO structure, with the distinct characteristic of 5 extra spots spacing equally between the central spot and the $(0001)_{\alpha\text{-Mg}}$ spot. The LPSO lamella was formed on $(0001)_{\alpha\text{-Mg}}$ habit plane of α-Mg matrix and grew or extended along $[01\bar{1}0]_{\alpha\text{-Mg}}$ direction of α-Mg matrix. Clearly, the LPSO lamella precipitated in α-Mg matrix belonged to the second type of LPSO structure.

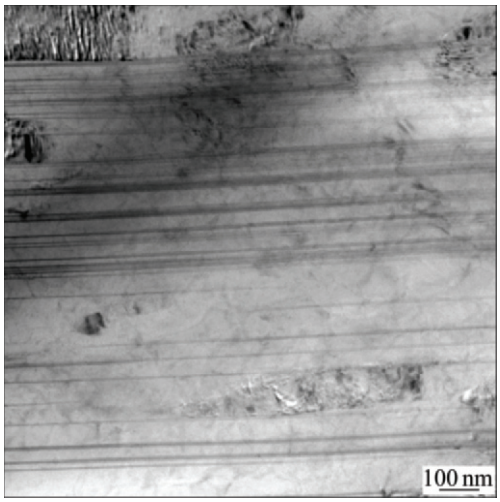

Fig. 3 TEM bright field image of lamellar structure

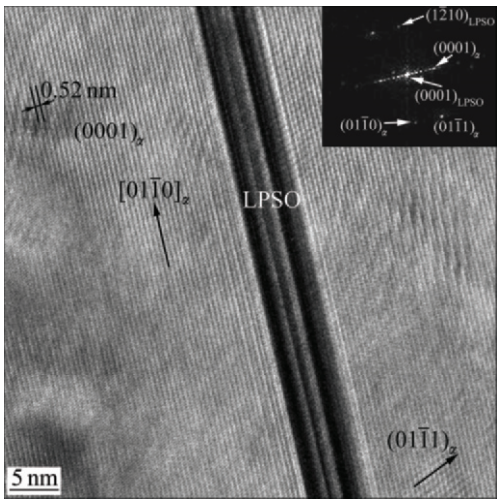

Fig. 4 HRTEM image and FFT pattern of lamellar LPSO structure observed inner α-Mg matrix of as-cast alloy (Incident electron beam direction was parallel to $[2\bar{1}\bar{1}0]_{\alpha\text{-Mg}}$)

Figure 5 showed the HRTEM image of the lamellar structure with width less than 5 nm. Two lamellas (A and B indicated by arrows) were observed as sharp linear contrasts parallel to $(0001)_{\alpha\text{-Mg}}$, the close-packed planes of the hexagonal Mg-matrix. Lamellas A and B can be considered to be formed by shearing the remaining planes above a close-packed plane by some displacement, as seen from the parallel lines in Fig. 4. According to the definition of the intrinsic stacking faults [29], lamellas A and B were actually the intrinsic stacking faults I_1 or I_2. Combining with the SAED pattern ($B=[2\bar{1}\bar{1}0]_{\alpha\text{-Mg}}$), we can get that the stacking faults also formed on $(0001)_{\alpha\text{-Mg}}$ habit plane of α-Mg matrix and grew or extended along $[01\bar{1}0]_{\alpha\text{-Mg}}$ direction of α-Mg matrix.

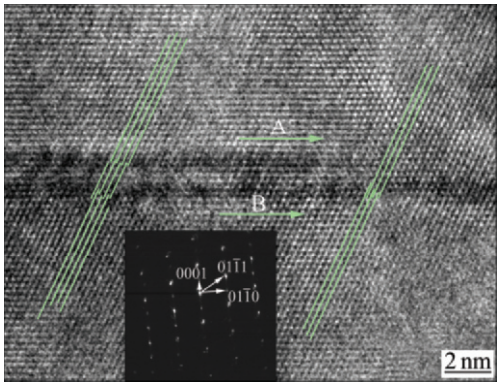

Fig. 5 HRTEM structure image and SAED pattern of stacking faults in alloy (Blue lines indicated closed-packed plane $(01\bar{1}1)$, incident electron beam direction was parallel to $[2\bar{1}\bar{1}0]_{\text{matrix}}$)

4 Discussion

In addition to the block-like LPSO phase (the first type), the LPSO lamella (the second type) accompanied by the stacking faults was observed in the as-cast Mg−Zn−Y−Zr alloy produced by conventional casting for the first time in this work. First principles calculations in this work showed that the addition of Y sharply decreased γ_{I_2} of the Mg−Zn−Y−Zr alloy while Zn just slightly increased γ_{I_2} of the Mg−Zn−Y−Zr alloy. Therefore, because the addition of Y can sharply decrease γ_{I_2} of Mg−Zn−Y−Zr alloy lots of stacking faults can be observed in the alloy.

The previous studies [7, 9] showed that the block-like LPSO distributed along grain boundaries and the interdendritic spacing in the as-cast alloys, and the LPSO phase precipitated inner the α-Mg solid solution grains only in the rapid solidified powder after hot extrusion [20]. However, experimental investigations in this work showed that the block-like LPSO distributed along grain

boundaries and the interdendritic spacing while the lamellar LPSO distributed in the α-Mg matrix simultaneously. This kind of distribution of LPSO was significant to the strength of the Mg−Zn−Y−Zr alloy, because the grain boundaries and the α-Mg matrix can be strengthened by LPSO distributed along grain boundaries and the LPSO lamella precipitated in α-Mg matrix simultaneously. It was worth to point out that LPSO as an effective strengthen phase was introduced into the α-Mg matrix without any severe rapid solidification condition and the following heat treatment at high temperature. In particular, the observation of the lamellar LPSO accompanied by stacking faults was a direct demonstration to the important role of stacking faults in formation of LPSO structure. It was found that there was an intimate connection between the stacking faults and the lamellar LPSO. First, the orientation relationship between the stacking faults and the α-Mg matrix was the same as that between the lamellar LPSO and the α-Mg matrix, and the lamellar LPSO structure and the stacking faults in Mg−Zn−Y−Zr alloy were both formed on $(0001)_{\alpha\text{-Mg}}$ habit plane and grew or extended along $[01\bar{1}0]_{\alpha\text{-Mg}}$ direction. Secondly, both of them had the same stacking sequence. The stacking sequence of the common intrinsic stacking faults of I_2 was ABABCACA [30], with the ABCA-type stacking sequence. It was demonstrated that the 18R-LPSO unit cell had three ABCA-type building blocks arranged in the same shear direction, while the 14H-LPSO unit cell had two ABCA-type building blocks arranged in opposite shear directions [19]. Therefore, from the stacking sequence point of view, LPSO structure was constructed from several I_2-type stacking faults. Based on these relationships between LPSO structure and stacking faults, it could be concluded that the stacking faults played a determinative role in formation of LPSO structure.

There were three kinds of ternary equilibrium phases in Mg−Zn−Y alloys in the Mg-rich region, which were X-phase ($Mg_{12}YZn$, LPSO structure), W-phase ($Mg_3Y_2Zn_3$, cubic structure) and I-phase (Mg_3YZn_6, icosahedral quasicrystal structure, quasi-periodically ordered) [31]. The previous investigation by our group showed that the formation of the secondary phases in Mg−Zn−Y−Zr alloys firmly depended on the mole ratio of Y to Zn and the equilibrium LPSO phase can be formed as the only secondary phase when the mole ratio of Y to Zn was more than 1.32 through phase diagram calculations [32]. The mole ratio of Y to Zn of the alloy (Mg-1.05Y-0.79Zn-0.07Zr (mole fraction, %)) in this work was 1.33, so the formation of LPSO first satisfied the criterion of the mole ratio of Y to Zn.

When the alloy is solidified, the segregation of Y and Zn may happen around the interdendritic space and grain boundary, which caused a decrease of SFE in these areas. As a result, stacking faults can be easily formed around the interdendritic spacing and grain boundary and the lamellar LPSO may nucleate through stacking faults and grows at certain temperature due to the slower cooling rate during the solidification.

The theory of nucleation directly through stacking faults was suggested by CHRISTIAN [33], OLSON et al [34] and HSU [35] for martensitic transformation. Here, a stacking fault was treated as a second-phase embryo. Based on the classical nucleation theory, the change of total free energy ΔG per unit area of stacking fault with a thickness of n planes can be expressed by

$$\Delta G = n[\Delta G^{\mathrm{Ch}} + \Delta G^{\mathrm{E}}] + 2\sigma(n) \tag{2}$$

where ΔG^{Ch} and ΔG^{E} were the chemical free energy change and elastic strain energy per unit area in a plane and defined as bulk thermodynamic quantities, and $\sigma(n)$ was the fault /matrix interfacial energy per unit area at n planes separation and was the only size-dependent quantity. Actually, $\sigma(n)$ was just the generalized stacking fault energy γ calculated by first principles method. Therefore, Eq. (2) can be modified to be:

$$\Delta G = n[\Delta G^{\mathrm{Ch}} + \Delta G^{\mathrm{E}}] + 2\gamma(n) \tag{3}$$

The embryo would grow up spontaneously when $\Delta G \leq 0$, so the numerical value of the chemical free energy change $|\Delta G^{\mathrm{Ch}}|$ was given by

$$\left|\Delta G^{\mathrm{Ch}}\right| \geq \Delta G^{\mathrm{E}} + \frac{2\gamma(n)}{n} \tag{4}$$

Equation (4) describes the relationship between the generalized stacking fault energy (γ) and the chemical driving force (ΔG^{Ch}) during nucleation of LPSO. It was shown that the stacking fault energy can directly affect the chemical driving force when the embryo of LPSO grew up, and the lower the stacking fault energy was, the smaller the chemical driving force needed to overcome the resistance, and the easier the embryo would grow up when n was a given value. So, as for the alloy with lower stacking fault energy, the nucleation directly through stacking fault would happen more easily. Therefore, the lower stacking fault energy with addition of Y was in favor of the formation of LPSO, and LPSO may nucleate directly through stacking faults from the thermodynamics point of view.

5 Conclusions

1) Addition of Y can sharply decrease the stacking fault energy of Mg−Zn−Y−Zr alloy, while Zn slightly increases the stacking fault energy of the alloy.

2) The block-like LPSO phase, the lamellar LPSO and stacking faults were observed simultaneously in the

as-cast Mg−Zn−Y−Zr alloy produced by conventional casting.

3) Stacking faults played a determinative role in formation of LPSO structure. The lamellar LPSO structure and stacking faults were both formed on $(0001)_{\alpha\text{-Mg}}$ habit plane and grew or extended along $[01\bar{1}0]_{\alpha\text{-Mg}}$ direction in Mg−Zn−Y−Zr alloy.

4) LPSO may nucleate directly through stacking faults and the lower stacking fault energy was in favor of formation of LPSO.

Acknowledgments

The authors are grateful to L Zhang and J C Lei for their kind help in TEM analysis and foil-specimen preparation.

References

[1] YANG Z, LI J P, ZHANG J X, et al. Review on research and development of magnesium alloys [J]. Acta Metallurgica Sinica: English Letters, 2008, 21(5): 313−328.

[2] ZHANG J, MA Q, PAN F S. Effects of trace Er addition on the microstructure and mechanical properties of Mg–Zn–Zr alloy [J]. Materials & Design, 2010, 31(9): 4043−4049.

[3] PAN F S, YANG M B. Preliminary investigations about effects of Zr, Sc and Ce additions on as-cast microstructure and mechanical properties of Mg–3Sn–1Mn (wt.%) magnesium alloy [J]. Materials Science and Engineering A, 2011, 528(15): 4973−4981.

[4] PAN F S, YANG M B, CHEN L. Effects of minor scandium on as-cast microstructure, mechanical properties and casting fluidity of ZA84 magnesium alloy [J]. Materials Science and Engineering A, 2010, 527(4/5): 1074−1081.

[5] PAN F S, LIU T T, ZHANG X Y, et al. Effects of scandium addition on microstructure and mechanical properties of ZK60 alloy [J]. Progress in Natural Science—Materials International, 2011, 21(1): 59−65.

[6] PAN F S, CHEN M B, WANG J F, et al. Effects of yttrium addition on microstructure and mechanical properties of as-extruded AZ31 magnesium alloys [J]. Transactions of Nonferrous Metals Society of China, 2008, 18(s): 1−6.

[7] KAWAMURA Y, YAMASAKI M. Formation and mechanical properties of $Mg_{97}Zn_1RE_2$ alloys with long-period stacking ordered structure [J]. Materials Transactions, 2007, 48(11): 2986−2992.

[8] YAMASAKI M, SASAKI M, NISHIJIMA M, et al. Formation of 14H long period stacking ordered structure and profuse stacking faults in Mg−Zn−Gd alloys during isothermal aging at high temperature [J]. Acta Materialia, 2007, 55(20): 6798−6805.

[9] YAMASAKI M, HASHIMOTO K, HAGIHARA K, et al. Effect of multimodal microstructure evolution on mechanical properties of Mg−Zn−Y extruded alloy [J]. Acta Materialia, 2011, 59(9): 3646−3658.

[10] DING W J, WU Y J, PENG L M, et al. Formation of 14H-type long period stacking ordered structure in the as-cast and solid solution treated Mg−Gd−Zn−Zr alloys [J]. Journal of Materials Research, 2009, 24(5): 1842−1854.

[11] HAGIHARA K, YOKOTANI N, KINOSHITA A, et al. Role of the microstructure on the deformation behavior in Mg12ZnY with a long-period stacking ordered structure [C]// Proceedings of Advanced Intermetallic-Based Alloys for Extreme Environment and Energy Applications, 2009: 329−334.

[12] MATSUMOTO R, YAMASAKI M, OTSU M, et al. Forgeability and flow stress of Mg-Zn-Y alloys with long period stacking ordered structure at elevated temperatures [J]. Materials Transactions, 2009, 50(4): 841−846.

[13] WU Y J, LIN D L, ZENG X Q, et al. Formation of a lamellar 14H-type long period stacking ordered structure in an as-cast Mg−Gd−Zn−Zr alloy [J]. Journal of Materials Science, 2009, 44(6): 1607−1612.

[14] YAMASAKI M, KAWAMURA Y. Thermal diffusivity and thermal conductivity of Mg−Zn−rare earth element alloys with long-period stacking ordered phase [J]. Scripta Materialia, 2009, 60(4): 264−267.

[15] HAGIHARA K, KINOSHITA A, SUGINO Y, et al. Effect of long-period stacking ordered phase on mechanical properties of Mg97Zn1Y2 extruded alloy [J]. Acta Materialia, 2010, 58(19): 6282−6293.

[16] HAGIHARA K, KINOSHITA A, SUGINO Y, et al. Plastic deformation behavior of Mg89Zn4Y7 extruded alloy composed of long-period stacking ordered phase [J]. Intermetallics, 2010, 18(5): 1079−1085.

[17] HAGIHARA K, YOKOTANI N, UMAKOSHI Y. Plastic deformation behavior of Mg12YZn with 18R long-period stacking ordered structure [J]. Intermetallics, 2010, 18(2): 267−276.

[18] SHAO X H, YANG Z Q, MA X L. Strengthening and toughening mechanisms in Mg−Zn−Y alloy with a long period stacking ordered structure [J]. Acta Materialia, 2010, 58(14): 4760−4771.

[19] ZHU Y M, MORTON A J, NIE J F. The 18R and 14H long-period stacking ordered structures in Mg−Y−Zn alloys [J]. Acta Materialia, 2010, 58(8): 2936−2947.

[20] KAWAMURA Y, HAYASHI K, INOUE A, et al. Rapidly solidified powder metallurgy $Mg_{97}Zn_1Y_2$ alooys with excellent tensile yield strength above 600 MPa [J]. Mater Trans, 2001, 42: 1172−1176.

[21] YAMASAKI M, ANAN T, YOSHIMOTO S, et al. Mechanical properties of warm-extruded Mg−Zn−Gd alloy with coherent 14H long periodic stacking bordered structure precipitate [J]. Scripta Materialia, 2005, 53(7): 799−803.

[22] ABE E, KAWAMURA Y, HAYASHI K, et al. Long-period ordered structure in a high-strength nanocrystalline Mg-1at%Zn-2at%Y alloy studied by atomic-resolution *Z*-contrast STEM [J]. Acta Materialia, 2002, 50(15): 3845−3857.

[23] CHINO Y, MABUCHI M, HAGIWARA S, et al. Novel equilibrium two phase Mg alloy with the long-period ordered structure [J]. Scripta Materialia, 2004, 51(7): 711−714.

[24] KRESSE G, FURTHMÜLLER J. Efficient iterative schemes for ab initio total-energy calculations using a plane-wave basis set [J]. Phys Rev B, 1996, 54(16): 11169−11186.

[25] PERDEW J P, WANG Y. Accurate and simple analytic representation of the electron-gas correlation energy [J]. Phys Rev B, 1992, 45(23): 13244−13249.

[26] BLÖCHL P E. Projector augmented-wave method [J]. Phys Rev B, 1994, 50(24): 17953−17979.

[27] CHETTY N, WEINERT M. Stacking faults in magnesium [J]. Phys Rev B, 1997, 569(17): 10844−10851.

[28] COURET A, CAILLARD D. An in situ study of prismatic glide in magnesium: II. Microscopic activation parameters [J]. Acta Met, 1985, 33(8): 1455−1461.

[29] YASI J A, LOUIS G, HECTOR J, et al. First-principles data for solid-solution strengthening of magnesium: From geometry and chemistry to properties [J]. Acta Materialia, 2010, 58(17): 5704−5713.

[30] HIRTH J P, LOTHE J. Theory of dislocations [M]. 2nd ed. New York: John Wiley & Sons, 1982: 354−359.

[31] LUO Z P, ZHANG S Q, TANG Y L, et al. Quasicrystals in as-cast Mg-Zn-RE alloys [J]. Scr Metall Mater, 1993, 28(12): 1513−1518.

[32] LUO S Q, TANG A T, PAN F S, et al. Effect of Y/Zn atom ratio on the phase constituent of Mg−Zn−Zr−Y alloys [J]. Trans Nonferrous Met Soc China, 2011, 21(4): 795−800.

[33] CHRISTIAN J W. A theory of the transformation in pure Co-balt [C]// Proc Royal Soc. London, 1951: 51−64.

[34] OLSON G B, COHEN M. A general mechanism of martensitic nucleation: Part I. General concepts and the FCC-HCP transformation [J]. Met Trans, 1976, 7A: 1897−1904.

[35] HSU T Y. Thermodynamics of martensitic transformation $\beta(\gamma)\rightarrow\varepsilon$ [J]. Acta Metall Sin, 1980, 16(4): 430−434. (in Chinese)